J Mater Sci (2007) 42:966–978
DOI 10.1007/s10853-006-0006-y

Effect of heating mode and temperature on sintering of YAG dispersed 434L ferritic stainless steel

S. S. Panda · A. Upadhyaya · D. Agrawal

Received: 22 August 2005 / Accepted: 14 March 2006 / Published online: 30 November 2006

Abstract This study examines the effect of heating mode, sintering temperature, and varying yttria alumina garnet (YAG) addition (5 and 10 wt%) on the densification and properties of ferritic (434L) stainless steel. The straight 434L stainless steel and 434L–YAG composites were sintered in a conventional and a 2.45 GHz microwave furnace. The composites were sintered to solid-state as well as supersolidus sintering temperature at 1200 and 1400 °C, respectively. Both 434L and 434L–YAG compacts coupled with microwaves and underwent rapid heating (~45 °C/min). This resulted in about 85% reduction in the processing time. For all compositions microwave sintering results in greater densification. As compared to conventional sintering, microwave sintered compacts exhibit a more refined microstructure, thereby, resulting in higher bulk hardness. The mechanical properties and sliding wear resistance of 434L stainless steel is shown to be sensitive both to the sintering condition as well as YAG addition and has been correlated to the effect of heating mode on the pore morphology.

S. S. Panda · A. Upadhyaya (✉)
Department of Materials and Metallurgical Engineering, Indian Institute of Technology, Kanpur, India
e-mail: anishu@iitk.ac.in

D. Agrawal
Materials Research Institute, The Pennsylvania State University, University Park, USA

Introduction

Powder metallurgical (P/M) stainless steels represent a small fraction of the total amount of P/M products across the world. However, attractive combination of excellent corrosion resistance, a wide range of strength levels including strength retention at cryogenic and elevated temperatures, good formability and aesthetically pleasing appearance have made P/M stainless steels the material choice for a range of applications [1]. For stainless steel, P/M route offers many advantages over conventional casting techniques, which include lower processing temperature, near-net shaping, high final density, greater material utilization (>95%) and a more refined microstructure that provides superior material properties [2]. Among various grades of P/M stainless steels used, austenitic grades are the most widely used for their corrosion resistance whereas ferritic stainless steels are more preferable for their magnetic and thermal properties [3]. In recent years, because of technological and economical advantages, ferritic stainless steels are gradually replacing austenitic steels. Typically, most stainless steel compacts are consolidated through solid-state sintering [4, 5]. Despite assuring higher dimensional stability of the component, solid-state sintering does not yield high densification due to presence of residual porosity. Several researchers [6–8] have examined the effect of sintering temperatures on the densification and mechanical properties of 434L ferritic stainless steel. However, nearly all the earlier reported sintering investigations have been conducted at temperatures ranging from 1,100 to 1,350 °C, which corresponds to solid-state sintering.

One approach for improving densification is by introducing liquid phase during the sintering process [9]. The formation of liquid phase enhances the diffusion kinetics and eliminates porosity, thereby, resulting in higher density. Liquid formation can be achieved by adding relatively low melting point elements such as Cu, Al and Sn [6, 7].

Despite densification enhancement, the above additives result in poor mechanical properties as they tend to segregate at the intergranular regions and form brittle phases [8, 9]. To overcome this, supersolidus liquid phase sintering (SLPS) is employed for consolidating single phase pre-alloyed powders [10–12]. In this process, compacts are heated in between the solidus and liquidus temperatures, causing formation of liquid phase preferentially at the grain boundaries [13]. The presence of liquid phase generally enhances densification by increasing diffusion kinetics. This, in turn, leads to particle fragmentation and subsequent repacking, which results in densification due to capillary stress induced particle rearrangement. As stainless steels powders are typically fabricated through atomization, they have pre-alloyed, single phase structure, and therefore, are amenable to supersolidus sintering.

In order to increase the mechanical and tribological properties, it is common to disperse fine particulates of borides, carbides and oxides in stainless steel. The effect of alumina (Al_2O_3), yttria (Y_2O_3), and silicon carbide (SiC) particulate additions on the densification, mechanical and tribological properties of solid-state sintered stainless steels have been extensively investigated [14–21]. Most of these dispersoids degrade densification during sintering, with few exceptions reported for austenitic stainless steel [14, 16, 17]. Patankar and Tan [16] observed that the addition of SiC to the 316L resulted in higher density in compacts sintered above 1,100 °C due to the chemical interactions between the stainless steel matrix and carbide to form a low melting eutectic (Fe–SiC). However, the brittleness of this phase resulted in deterioration in the mechanical properties. Elsewhere, Datta and Upadhyaya [17] reported that 3 wt% CrB addition to 316L resulted in higher sintered density. Unlike austenitic stainless steel, very little investigation has been conducted on the effect of dispersoids addition on the sintering behavior of ferritic stainless steel. Mukherjee and Upadhyaya [19] investigated the effect of Al_2O_3 addition on 434L ferritic stainless steel. Al_2O_3 addition has been shown to increase the wear resistance, but it adversely affects densification and mechanical properties. In contrast, Y_2O_3 addition in optimal amount has shown to enhance densification of stainless steel compacts. This was attributed to the interaction of Cr_2O_3 with the Y_2O_3 dispersoids. Furthermore, it was observed that the porosity was more homogeneous for the Y_2O_3 containing composites than for the pure 434L under identical sintering condition [15]. Recently, Shankar et al. [20] systematically examined the effect of varying yttria (Y_2O_3) content on the densification response of ferritic stainless steel. They reported that the sintered density is enhanced by the addition of yttria to 434L ferritic stainless steel. For cost effectiveness, Jain et al. [21] have proposed the use of mixed oxides of yttria and alumina as additives. Recently, they have reported that yttrium aluminium garnet (YAG) addition does not degrade densification of stainless steel compacts both in solid-state as well as supersolidus sintering conditions.

One of the limitations of using higher sintering temperature and conventional heating mode is microstructural coarsening. Typically, most of heating occurs radiatively during sintering in a conventional (electrically heated) furnace. Consequently, to prevent thermal gradient within the compact, a slower heating rate coupled with isothermal hold at intermittent temperatures is provided, which increases the process time. In recent years, materials are being increasingly heated using microwaves [22, 23]. Microwaves are the electromagnetic waves that have a frequency range around 0.3–300 GHz with corresponding wavelengths ranging from 1 m to 1 mm. When electromagnetic (EM) energy is applied to a material some of it is reflected by the surface of the material, some are transmitted through the material and rest are absorbed within the material. This last characteristic is important when using EM energy for processing. In the microwave frequency range, the absorption properties of non-metallic materials vary greatly and depend on the dielectric properties. Microwaves directly interact with the particulates within the pressed compacts and thereby provide rapid volumetric heating. This reduces processing time and results in energy saving. In addition, the uniform heating minimizes problems such as localized microstructural coarsening and results in improved properties [24]. Until recently, most of the microwave sintering was restricted to ceramic materials and cemented carbides [25]. Recently, it was shown that metals too could couple with microwaves provided they are in powder form rather than monolithic [26]. Subsequently, microwave sintering of steel powder compact was conducted [27, 28]. More recently, it has been shown that bronze and steel powder compacts too couple with microwaves and can be effectively sintered [29]. Though there have been attempts to explain microwave heating of metal powders, still there is not yet any consensus on a comprehensive theory to explain the mechanism [30].

The present study investigates the microstructural, densification, mechanical, and tribological property response in straight 434L and 434L–YAG composites consolidated using both microwave as well as conventional furnace sintering through solid-state and supersolidus sintering routes.

Experimental procedure

The as-received gas-atomized 434L ferritic stainless steel (supplier: Ametek Specialty Metal Products, USA) and YAG (supplier: Treibacher, Austria) powders had an average size of 60 and 1.5 μm, respectively. The nominal composition of the as-received powders are presented in Table 1. The powder characteristics are summarized in Table 2. The two powders were mixed in the required proportions (5 and 10 wt% of YAG) in a turbula mixer (model: T2C, supplier: Bachoffen, Switzerland) for 20 min. The mixed powders were uniaxially compacted at 600 MPa in a 50T hydraulic press (model: CTM-50, supplier: FIE, lchalkaranji, India) with floating die. To minimize friction, compaction was carried out using zinc stearate as a die wall lubricant. The stainless steel compacts (straight as well as YAG containing ones) were pressed to a green densities ranging between 80 and 82%. The sintering response on densification and microstructures were evaluated on cylindrical pellets (16 mm diameter and 6 mm height). For measuring the tensile properties, flat tensile bars were pressed as per MPIF standard 10 [31].

The green (as-pressed) compacts were sintered using conventional and microwave furnace. The conventional sintering of green compacts were carried in a $MoSi_2$ heated horizontal tubular sintering furnace (model: OKAY 70T-7, supplier: Bysakh, Kolkata, India) at a constant heating rate of 5 °C/min. To ensure uniform temperature distribution during heating, intermittent isothermal hold for 15–30 min was provided at 500, 750, and 1,000 °C. The compacts were sintered in solid-state and supersolidus condition at 1,200 and 1,400 °C, respectively. Sintering was carried out for 60 min in hydrogen atmosphere with dew point –35 °C. Microwave sintering of the green compacts was carried out using a multi-mode cavity 2.45 GHz, 6 kW commercial microwave furnace (model: RC/20SE, supplier: Amana Radarange). Unlike a conventional furnace, the temperature of the samples inside a microwave furnace cannot be monitored using a thermocouple. The presence of thermocouples can locally distort the electromagnetic field and can even lead to measurement errors [32]. The temperature of the sample was monitored using an infrared pyrometer (Raytek, Marathon Series) with the circular cross-wire focused on the sample cross-section. The pyrometer is emissivity based; therefore temperature could not measure temperature below 700 °C [33]. Hence, for the temperature measurements for all the compacts was done by considering emissivity of steel (0.35) [34]. Typically, emissivity varies with temperature. However, as very little variation in the emissivity was reported in the temperature range used in the present study, hence, the effect of variation in emissivity was ignored in the present investigation. Further details of the experimental setup of microwave sintering are described elsewhere [28, 29]. In order to ensure repeatability and reproducibility for each condition, four compacts were sintered.

The sintered density was obtained by dimensional measurements and the average values and standard deviation was evaluated. The sintered compacts were polished to mirror finish and ultrasonically cleaned in acetone, followed by etching in Marvels reagent (12 g $CuSO_4 \cdot 5H_2O$—60 ml HCl—60 ml distilled water). The microstructural analyses of the samples were carried out through optical microscope (model: Q5001W, supplier: Leica Imaging System Ltd., Cambridge, UK). Both the pore size and shape factor distribution

Table 2 Characteristics of the powders in as-received conditions used in the present study

Property	Powder	
	434L	YAG
Processing technique	Gas atomization	Chemical reduction
Powder shape	Spherical	Rounded
Cumulative powder size, μm		
D_{10}	8.5	0.5
D_{50}	35.3	1.5
D_{90}	75.1	2.1
Apparent density, g/cm^3	2.6	0.70
Flow rate, s/50 g	28	98
Theoretical density, g/cm^3	7.86	4.50

Table 1 Nominal composition (in wt%) of the as-received 434L and YAG powder used in the present study

Powder	Cr	Mo	Si	Mn	C	S	P	Fe	Y	Al	Ti
434L	17	1.0	0.71	0.2	0.023	0.02	0.02	Bal.	–	–	–
YAG	–	–	0.014	–	0.08	–	–	0.014	45.05	22.5	<0.01

were determined from the optical micrographs of the unetched straight 434L compacts. The pore size was estimated by measuring the pore area, while pore shape was characterized using a shape-form factor, F, which is related to the pore surface area, A, and its circumference in the plane of analysis, P, as follows [35]:

$$F = \frac{4\pi A}{P^2}. \quad (1)$$

Both pore area distribution and shape factor was directly measured using image analyzer. The shape factor of a feature is inversely proportional to its roundness. A shape factor of 1 represents circular pore in the plane of analysis and as it reduces the pores tend to become more irregular. The sintered grain size of the stainless steel and stainless steel–YAG compacts was measured using intercept method [35].

Vickers bulk hardness measurements were performed on the samples at 2 kg load. The observed hardness values are the averages of five readings taken at random spots throughout the sample. The tensile test was conducted only for supersolidus sintered stainless steel compacts using a 10 kN capacity Universal Testing Machine at a constant cross-head speed 0.5 mm/min. From the tensile curves, the ultimate tensile strength and ductility were determined. In order to ensure repeatability, for each condition, four samples were evaluated. To correlate the tensile properties with the microstructure, fractography analyses of the samples were carried out using SEM imaging (model: JSM-840A, supplier: JEOL, Japan).

The tribological response of the supersolidus sintered 434L stainless steel and 434L–YAG composites were measured using a pin-on-disc wear tester (model: TR20, supplier: Ducom, Bangalore, India) at a load of 50 N and sliding velocity of 2 m/s. The wear tracks were analyzed using scanning electron microscope.

Results and discussion

Heating profiles

Figure 1 compares the thermal profiles of the compacts—for both solid-state as well as supersolidus sintering—heated in conventional and microwave furnace. It is interesting to note that both straight as well as YAG-added 434L compacts couple with microwaves and get heated up rapidly. In case of microwave heating, temperature could only be measured from 700 °C onwards. However, it takes about 5.5 min to heat up the compacts from room temperature to 700 °C. The overall heating rate in microwave furnace was around 45 °C/min. Ignoring the isothermal holds at intermittent temperatures in conventional furnace, there is about 85% reduction in the process time during sintering of stainless compacts in microwave furnace.

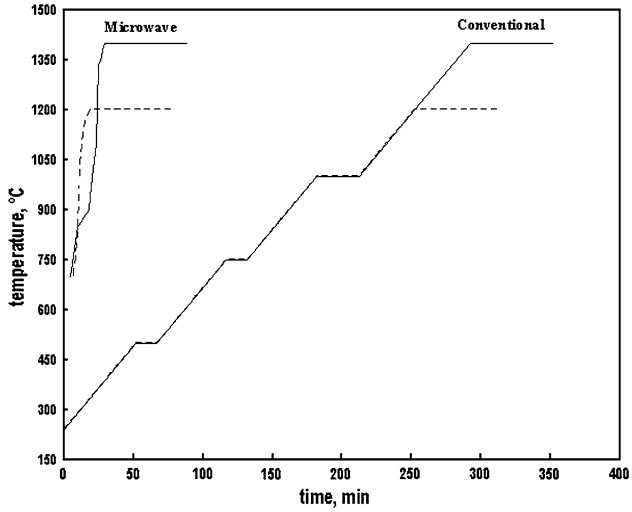

Fig. 1 Comparison of conventional and microwave sintering cycles for compacts heated to 1,200 and 1,400 °C

Microwave heating in metals is different than that observed in dielectric materials (mostly ceramics). Being good conductors, no internal electrical field is induced in metals. The induced electrical charge remains at the surface of the sample. As a consequence, monolithic metals reflect microwaves; hence no bulk absorption (heating) occurs, particularly, at temperatures below 500 °C. Microwaves interaction with metals is restricted to its surface only. This depth of penetration in metals, also known as skin-depth (δ), is defined as the distance into the material at which the incident power drops to $1/e$ (36.8%) of the surface value. The skin depth is mathematically expressed as follows:

$$\delta = \frac{1}{\sqrt{\pi f \mu \sigma}} = 0.029\sqrt{\rho \lambda_0} \quad (2)$$

where f is microwave frequency (2.45 GHz), μ is magnetic permeability, σ is electrical conductivity, ρ is electrical resistivity, λ_0 is incident wavelength (12.24 cm for 2.45 GHz waves). The skin-depth in metals typically varies between 0.1 and 10 μm and is inversely related to the electrical conductivity. For metallic system, as the resistivity increases with increase in temperature, the skin depth too increases. In metal powders, the surface area and thereby the

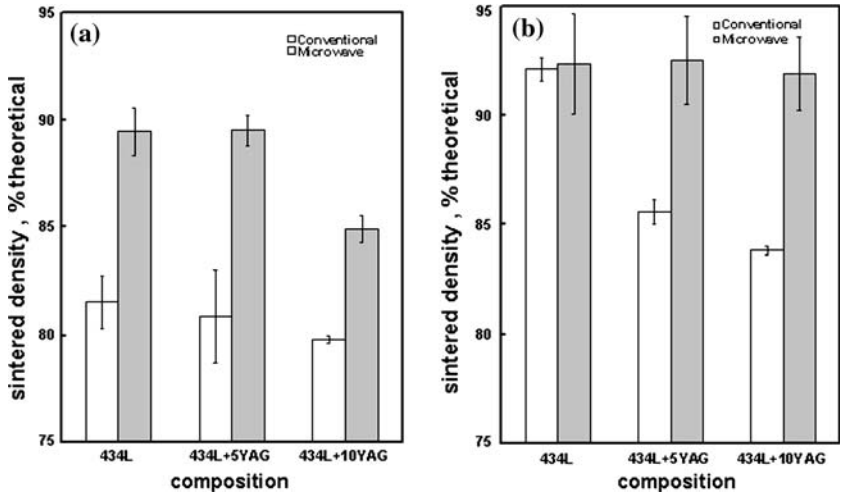

Fig. 2 Effect of YAG addition on the density of ferritic stainless steel sintered in conventional and microwave furnace at (**a**) 1200 °C and (**b**) 1,400 °C

''effective skin'' (portion of metal powder that couples with microwaves) is high enough to contribute to its heating. The skin depth of the metal plays an important role in governing the power loss during the microwave–metal interaction which leads to its heating [24]. Recently, Mishra et al. [36] have proposed a model for predicting heating of particulate metal compacts in microwaves. Their approach incorporates microwave heating of particulate metals by solving Maxwell's equations of electromagnetism simultaneously with the heat transfer equation.

Densification response

Figure 2a, b show effect of YAG addition and heating mode on the sintered density of 434L compacts at 1,200 and 1,400 °C, respectively. It is evident that as compared to 1,200 °C, both the straight 434L as well as 434L–YAG compacts exhibit higher density at 1,400 °C. This is attributed to the melt formation at higher temperature which promotes densification by enhancing diffusion kinetics. The stainless steel powders used in the present study were prepared by gas-atomization and hence were in pre-alloyed form. Unlike conventional liquid phase sintering, wherein a lower melting constituent is required, the pre-alloyed powders themselves undergo partial melting during supersolidus sintering [11–13]. Furthermore, during supersolidus sintering, melt forms preferentially at grain boundaries and thus is homogeneously distributed. This results in enhanced densification through capillary induced pore-filling and grain rearrangement [12]. It is interesting to note that both straight 434L and 434L–YAG composites, sintered in microwaves exhibit much better density. Though at 1,400 °C the compacts show higher sintered density (>90%) than 1,200 °C, the difference is narrow as compared to that of conventional sintering. This further confirms that both straight 434L as well as 434L–YAG composites effectively couple with microwaves. Due to this coupling, addition of YAG enhances the density as compared to conventional sintering where its addition degrades the densification properties. The microwave sintered straight 434L compacts show a large improvement in density at 1,200 °C (Fig. 2a) over their conventionally sintered counterparts, whereas, at 1,400 °C, it exhibits almost the same sintered density with a variation of hardly 0.1% (Fig. 2b). It may be due to removal of almost all pores at supersolidus temperature enhancing the densification. The YAG particles, being ceramic in nature, provide an effective pathway for microwave absorption, which makes the stainless steel–YAG composites more amenable to microwave sintering. As compared to 1,200 °C, there is no significant change in densification on addition of YAG to 434L stainless steel at 1,400 °C. The enhanced densification in microwave sintered compacts can be attributed to the fast heating rate, which restricts grain coarsening [37]. This was confirmed by quantifying the microstructure of matrix (434L) as a function of sintering temperature, YAG addition and heating mode (Table 3). It is quite

Table 3 Effect of sintering temperature and sintering mode on the average grain size of the 434L and 434L–YAG compacts

Composition	Average grain size, μm			
	1,200 °C		1,400 °C	
	C	M	C	M
434L	90	70	170	120
434L–5YAG	55	50	75	70
434L–10 YAG	45	40	65	57

C, conventionally sintered; M, microwave sintered

evident from Table 3, that microwave sintering restricts coarsening. Consequently, grain boundary diffusion is expected to be more pronounced in microwave sintering. Elsewhere, Sahay and Krishnan [38, 39] have shown a log-linear relationship between the heating rate and the activation energy for crystallization for glass ($Se_{71}Te_{20}Sb_9$ and $Ge_{20}Te_{80}$) and linear aromatic polyester systems. This relationship has been attributed to the increase in the free energy under isochronal condition, which effectively decreases the apparent activation energy at higher heating rates. It is envisaged that activation energy during microwave sintering too follows similar trend, thereby, leading to enhanced densification. Recently, Porada and Park [27] have shown diffusional enhancement during microwave heating. To corroborate this in P/M stainless steel, future work should aim at comparing the densification response of ferritic stainless steel compacts under microwave and fast-heating furnace at equivalent heating rates.

From Fig. 2, it is evident that YAG addition reduces densification for compacts sintered conventionally at 1,200 °C as well as 1,400 °C. At higher level of YAG the dispersoids behaves predominantly as an inert additive, thus lowering the diffusion rate and densification. The fine YAG particles favor the possibility of YAG–YAG interactions and thereby formation of YAG agglomerates along grain boundaries. This results in reduction of stainless steel–YAG interaction and subsequent poor

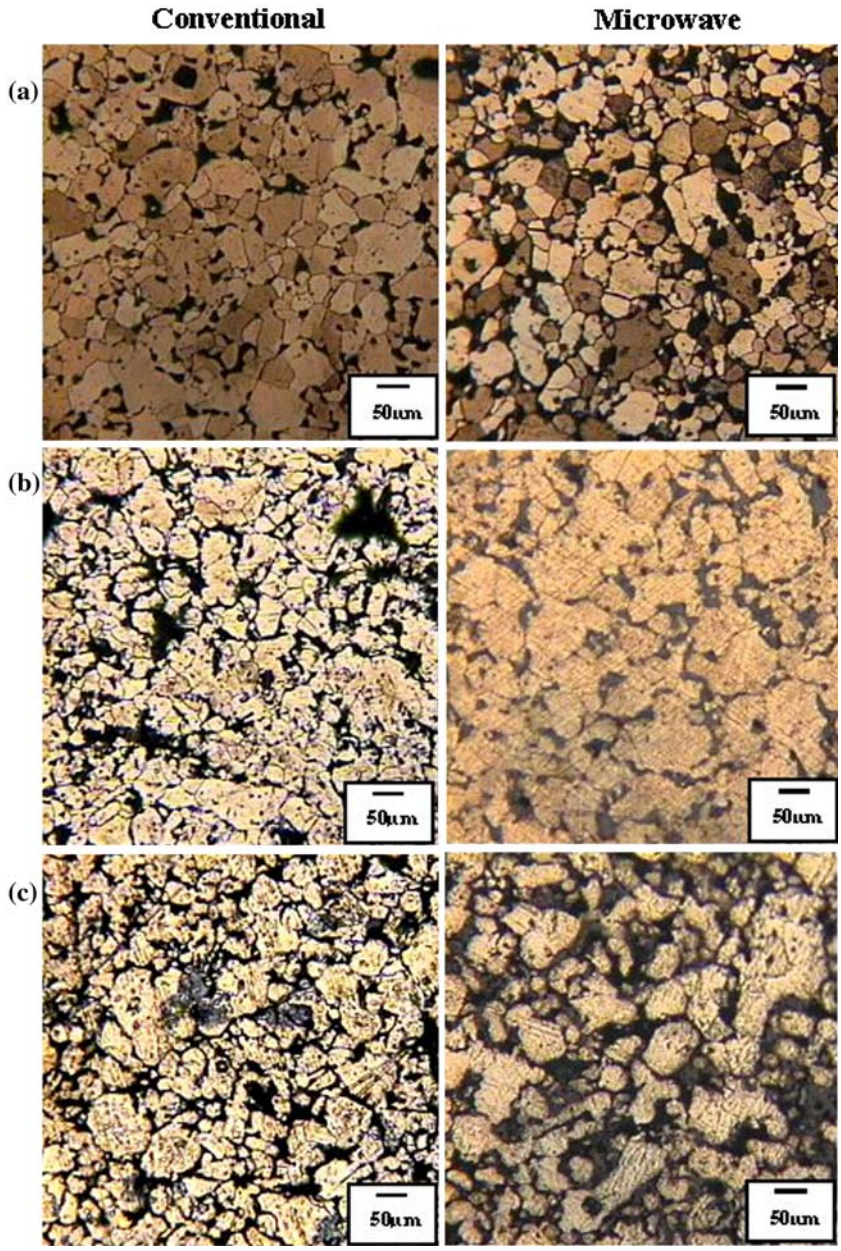

Fig. 3 Optical micrographs of (**a**) 434L, (**b**) 434L + 5YAG, and (**c**) 434L + 10YAG compacts sintered at 1,200 °C for 1 h in conventional (left) and microwave (right) furnace

sinterability. This is conformity with the observation by Mukherjee and Upadhyaya [19] and others [14, 17–19]. In contrast to the conventional heating, an optimal YAG addition results in densification enhancement during microwave sintering. For both solid-state as well as supersolidus condition, 434L–5YAG composites exhibit highest densification during microwave sintering (Fig. 2). This can be attributed to the interaction of the microwaves with the YAG particles. It is hypothesized that the YAG particles get heated up differentially and more effectively than the stainless steel powders, which may further contribute to densification enhancement by providing localized *hot spots*. Elsewhere, Peelamedu et al. [40] too observed differential microwave heating effects in multi-component systems and termed such phenomenon as anisothermal sintering. They have shown that the anisothermal heating results in densification enhancement during sintering. In 434L–YAG composites, however, an optimal addition (5 wt%) of YAG contributes most to the compact densification. In case of higher YAG content (10 wt%) because of the fine particle size of YAG, there is a likelihood of YAG–YAG interaction and agglomeration which causes a decrease in sintered density. However, a more detailed investigation is required to further optimize the YAG content.

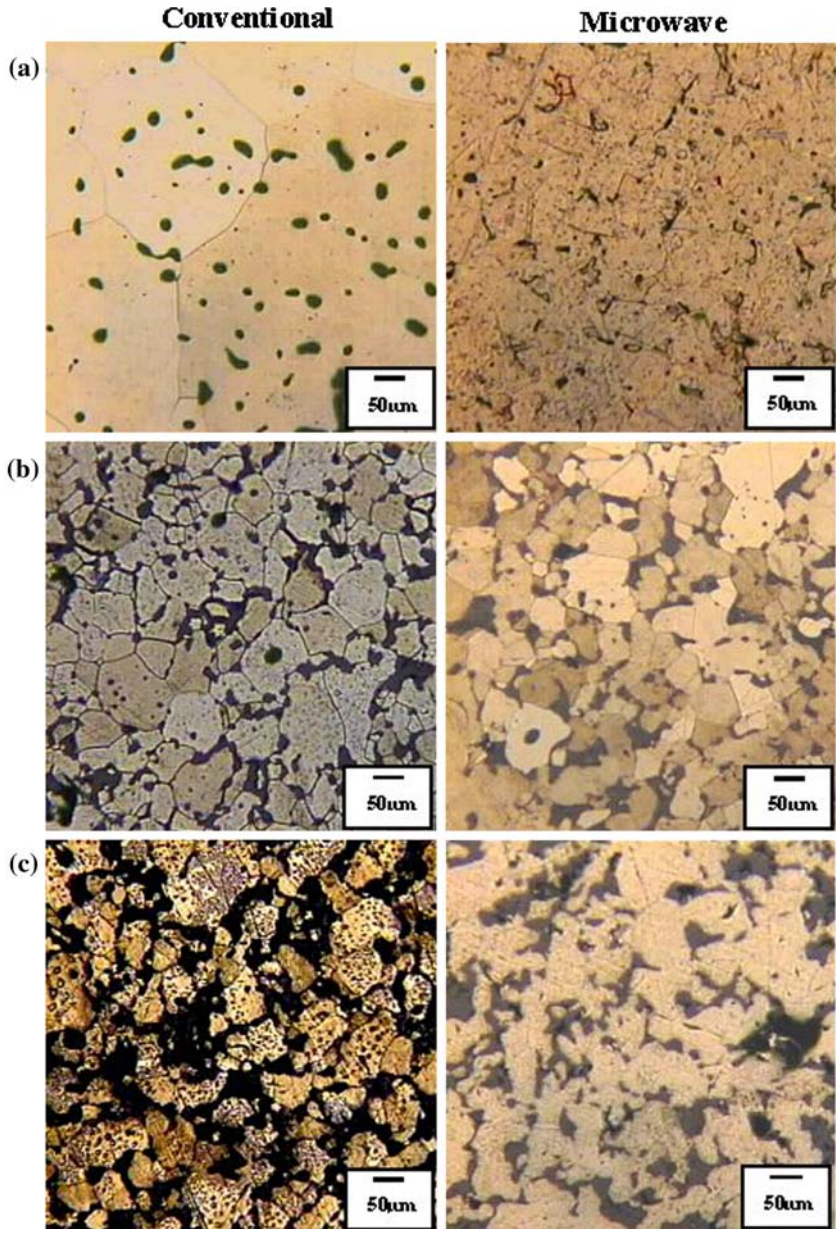

Fig. 4 Optical micrographs of (**a**) 434L, (**b**) 434L + 5YAG, and (**c**) 434L + 10YAG compacts sintered at 1,400°C for 1 h in conventional (left) and microwave (right) furnace

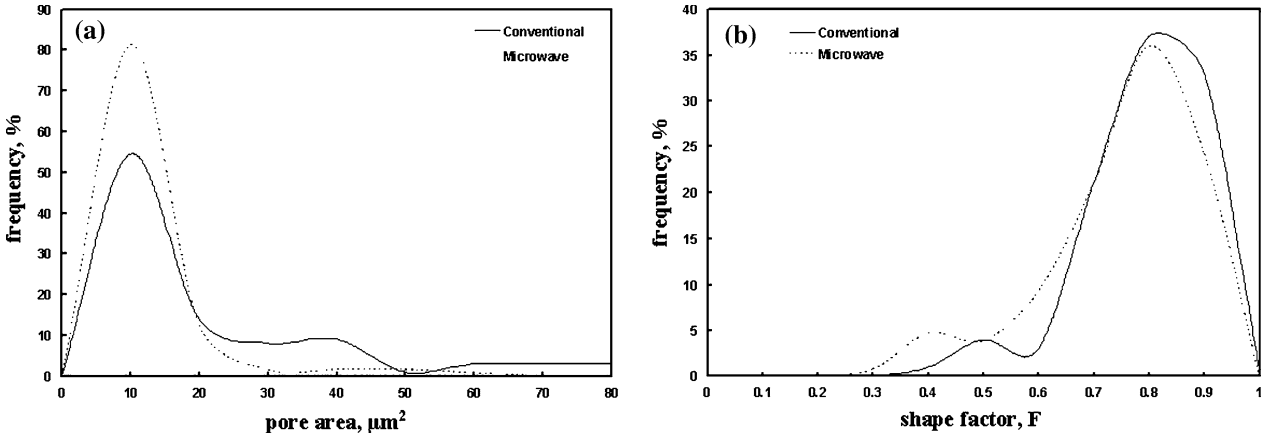

Fig. 5 Comparison of (**a**) pore area distribution and (**b**) shape factor distribution of the ferritic stainless steel compacts sintered in conventional and microwave furnace

Microstructure and pore evolution

Figures 3, 4 compare the optical micrographs of conventional and microwave sintered compacts of straight 434L and 434L–YAG composites. It is quite evident from both figures that compacts sintered at higher temperature exhibit microstructural coarsening, which is more pronounced in conventionally sintered compacts. Table 3 compares the effect of sintering temperature and heating mode on the matrix (434L) grain size stereologically quantified using intercept method. It is evident that as compared to solid-state sintering, supersolidus sintering results in greater microstructural coarsening. Clearly, microwave sintering and YAG addition restricts grain growth. The sintered microstructure reveals large and irregular pores predominantly along grain boundaries in the solid-state sintered stainless steels. The pores become more rounded and smaller but intergranular when processed via supersolidus liquid phase sintering. During supersolidus sintering, the melt formation promotes coarsening. For both microwave and conventional sintering, YAG addition restricts microstructural coarsening. As evidenced from Figs. 3 and 4b, c, YAG dispersoids remain preferentially segregated at the 434L inter-particle interfaces, thereby, restricting grain growth and the pores remain intergranular.

The optical micrographs of compacts (Figs. 3, 4) reveal distinct differences in the pore morphology of microwave compacts vis a vis their conventional counterparts. For both straight stainless steel as well as stainless steel–YAG composites the pores have rounded appearance in both conventional. This was verified by quantifying and comparing the distribution of pore sizes (measured as area) and shape factors of conventional and microwave sintered compacts. As subsequent mechanical properties of only the supersolidus sintered compacts were compared, hence the pore measurement was done only for 1,400 °C sintered compacts. Furthermore, this exercise was limited to straight 434L compacts only, as in case of YAG containing composites, it was difficult to distin-

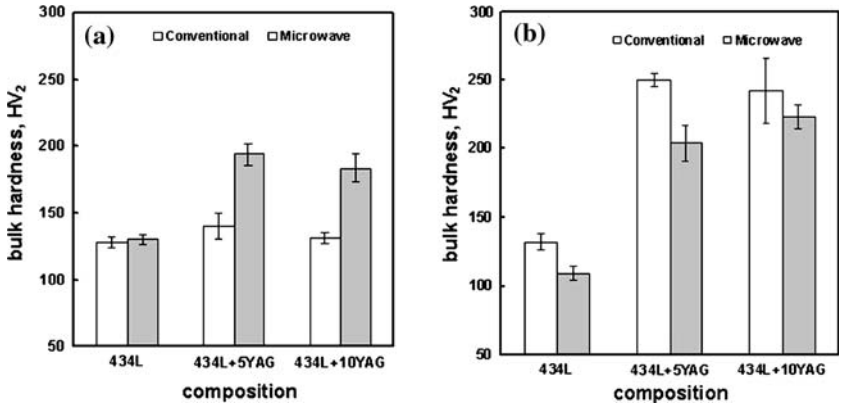

Fig. 6 Effect of YAG addition and sintering condition on the bulk hardness of 434L compacts sintered in conventional and microwave furnace at (**a**) 1,200 °C and (**b**) 1,400 °C

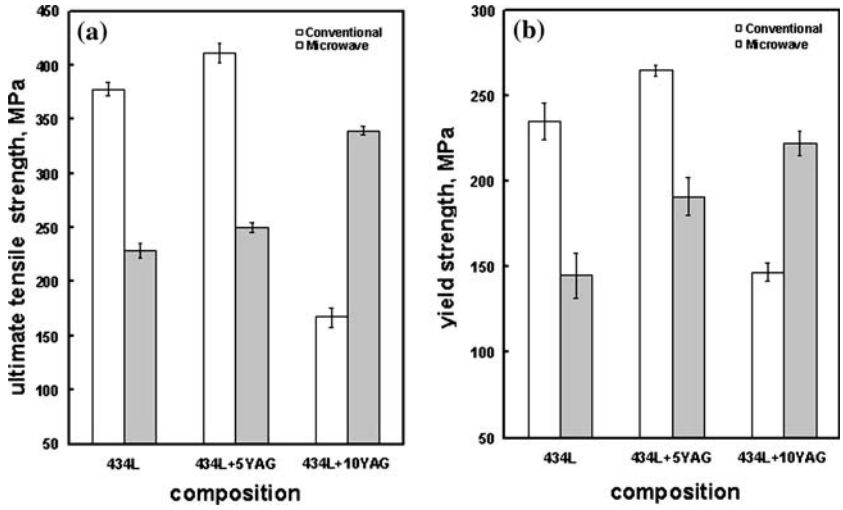

Fig. 7 Effect of YAG addition and sintering mode on the (**a**) ultimate tensile strength and (**b**) yield strength of 434L compacts sintered in conventional and microwave furnace at 1400 °C

guish between YAG and porosity in the optical micrographs. Figure 5a, b compare the pore area and shape factor distribution of conventionally and microwave sintered 434L compacts. From Fig. 5a, it is obvious that as compared to conventional sintering, the pores in the microwave sintered 434L are not only smaller but also have a narrower distribution. On comparing the respective shape factor distribution (Fig. 5b), the porosity in the microwave sintered compacts appear skewed towards lower shape factor values, which is indicative of relatively irregular pores. This could be attributed to the faster processing cycle, which does not yield sufficient time for proper pore rounding. This is in contrast with recent observations by Anklekar et al. [41] who have reported relatively more rounded pore morphology in microwaves sintered Fe–2Cu–0.8C steels. While the pore area variation is narrower in microwave sintered compact—with most pores having below 10 μm^2 area—the shape factor shows steep variation with most clustering in between 0.5 and 0.8. The conventionally sintered 434L compacts exhibit more regular pore morphology in between 0.7 and 0.8 despite a wider variation in the pore area.

Mechanical properties

Figure 6a, b show the effect of YAG addition on the hardness of ferritic stainless steels sintered in conventional and microwave furnaces. For straight 434L compacts sintered at 1,200 °C, the bulk hardness is higher than those reported by Iglesias et al. [42] which were compacted at much higher pressure (700 MPa) and sintered at 1,250 °C. The bulk hardness of 434L samples from the present study are even higher than those reported by Mukherjee and Upadhyaya [19] on the same grade and sintered at 1,200 and 1,350 °C. For both conventional and microwave sintering in both solid-state as well as supersolidus conditions, the hardness of compact increases with YAG addition. This may be due to more matrix–particle interaction. In case of compacts consolidated at 1,200 °C, the hardness of microwave sintered compact is higher. This

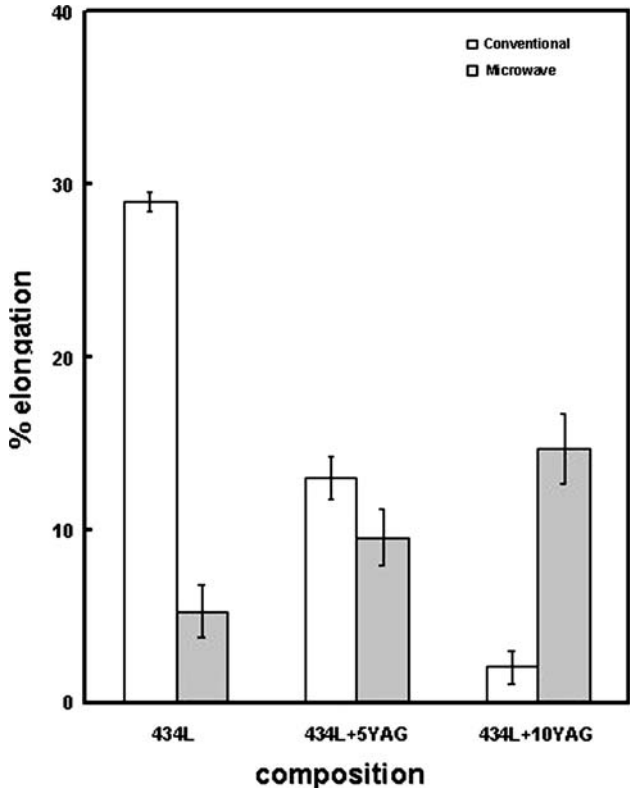

Fig. 8 Effect of YAG addition and sintering mode on the ductility of 434L compacts sintered in conventional and microwave furnace at 1,400 °C

is due to higher densification of microwave sintered 434L and 434L–YAG compacts (Fig. 2a). Despite an increase in the sintered density at higher temperatures, it is interesting to note that the hardness of the microwave sintered compacts is lower than their conventional counterparts at 1,400 °C. The reason for this behavior is not clear. In case of conventional sintering, YAG addition increases bulk hardness, despite an overall decrease in the compact sinterability. From the microstructural observations, it is evident that YAG remains segregated at the grain boundaries. This restricts microstructural coarsening, thereby, resulting in hardness increase. Furthermore, the high inherent hardness of YAG particulate negates the effect of poor densification in lowering the bulk hardness. Just like conventional sintering, the hardness of microwave 434L–YAG composite is higher than straight 434L compacts. However, unlike conventional sintering, an optimal YAG addition of 5 wt% results in maximum hardness in 1,200 °C whereas 10 wt% YAG addition in stainless steel at 1,400 °C results highest hardness. This is in accordance with the sintered density trend as shown in Fig. 2a, b, wherein the 434L–5YAG compacts have highest density at solid-state microwave sintering and at supersolidus sintering YAG addition has almost same effect that of straight 434L stainless steel exhibiting highest density of more than 90% theoretical.

Figure 7a, b compare the mechanical strength (UTS and YS) of 434L and 434L–YAG compacts sintered at 1,400 °C using both conventional as well as microwave furnace. The strength and ductility of conventionally sintered stainless steel in the present study is much higher than those reported elsewhere [19, 42]. This

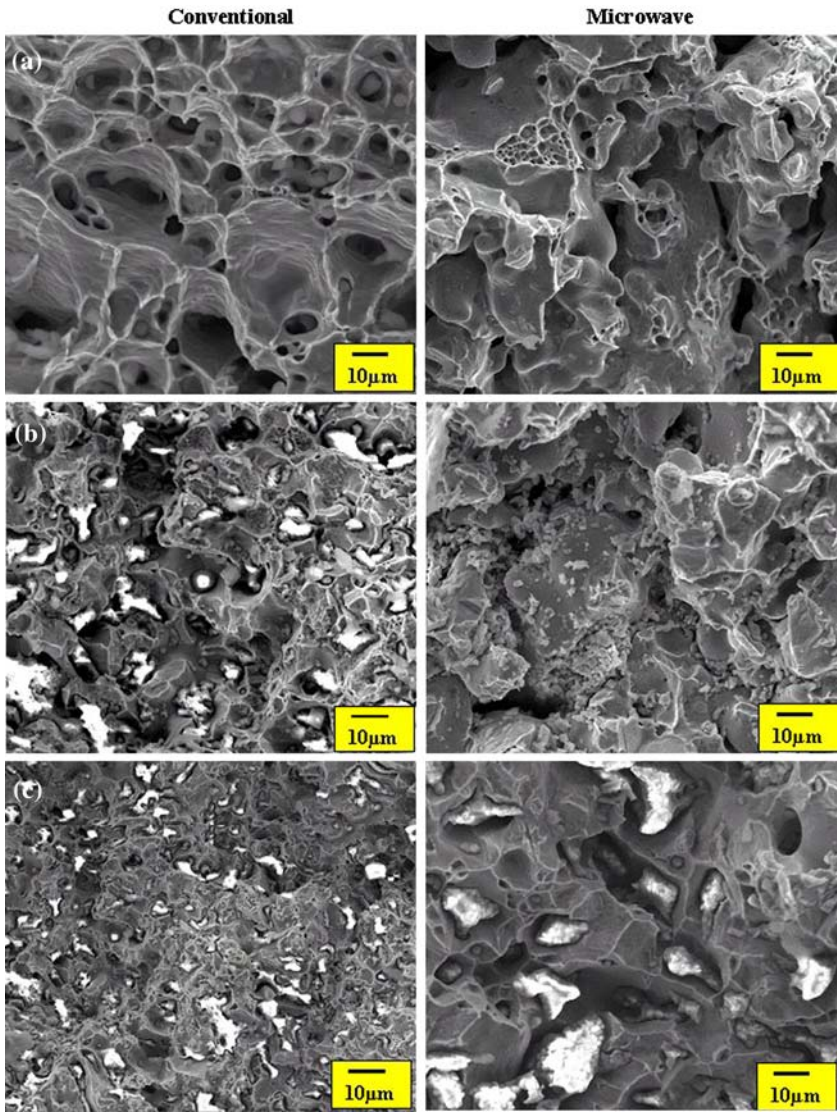

Fig. 9 SEM fractographs of (**a**) 434L, (**b**) 434L + 5YAG, and (**c**) 434L + 10YAG compacts sintered at 1,400 °C in conventional (left) and microwave (right) furnace and subjected to tensile test

underscores the importance of processing stainless steels in supersolidus region. The strength of microwave sintered compacts increases on addition of YAG and is similar to that of hardness (Fig. 7b) and correlates well with the densification (Fig. 2b). Interestingly, the ductility (Fig. 8) of microwave sintered compact increases with increasing YAG content, whereas it progressively decreases in case of conventionally sintered compacts. However, as compared to microwave sintering both the strength as well as the ductility of conventionally sintered straight 434L and 434L–5YAG composite are higher. This trend is in contrast to recent observations by Anklekar et al. [41] on Fe–Cu–C steels wherein microwave sintered compacts exhibited higher strength as well as ductility. However, microwave sintering results in higher strength and ductility for 434L–10YAG compacts.

Figure 9 shows representative fractographs of conventional and microwave sintered ferritic stainless steel both with and without YAG addition. Conventionally sintered 434L show distinct dimpled morphology which is characteristic of ductile failure (Fig. 9a). In contrast, the microwave sintered compacts fail through intergranular decohesion for both straight 434L stainless steel and 434L–5YAG composites. This is attributed to the elongated pore morphology (Figs. 3–5), which act as stress-concentration sites and lead to premature, brittle failure at relatively lower load. Unlike conventional sintering, the stainless steel matrix of microwave sintered 434L–10YAG compacts show necking and dimpling (Fig. 9c), which indicates relatively ductile fracture mode. Consequently, microwave sintering results in higher strength and ductility in 434L–10YAG compacts. This can be attributed to the higher densification (Fig. 2b) and relatively lesser growth (Table 3) in microwave sintered 434L–10YAG compacts. In case of conventional sintering, an increase in YAG content, changes the fracture mode from dimpled to intergranular mode, thereby resulting in lowering of ductility. This is attributed to lowering of sinterability with YAG addition (Fig. 2) and the presence of brittle additive phase at the 434L interparticle interface.

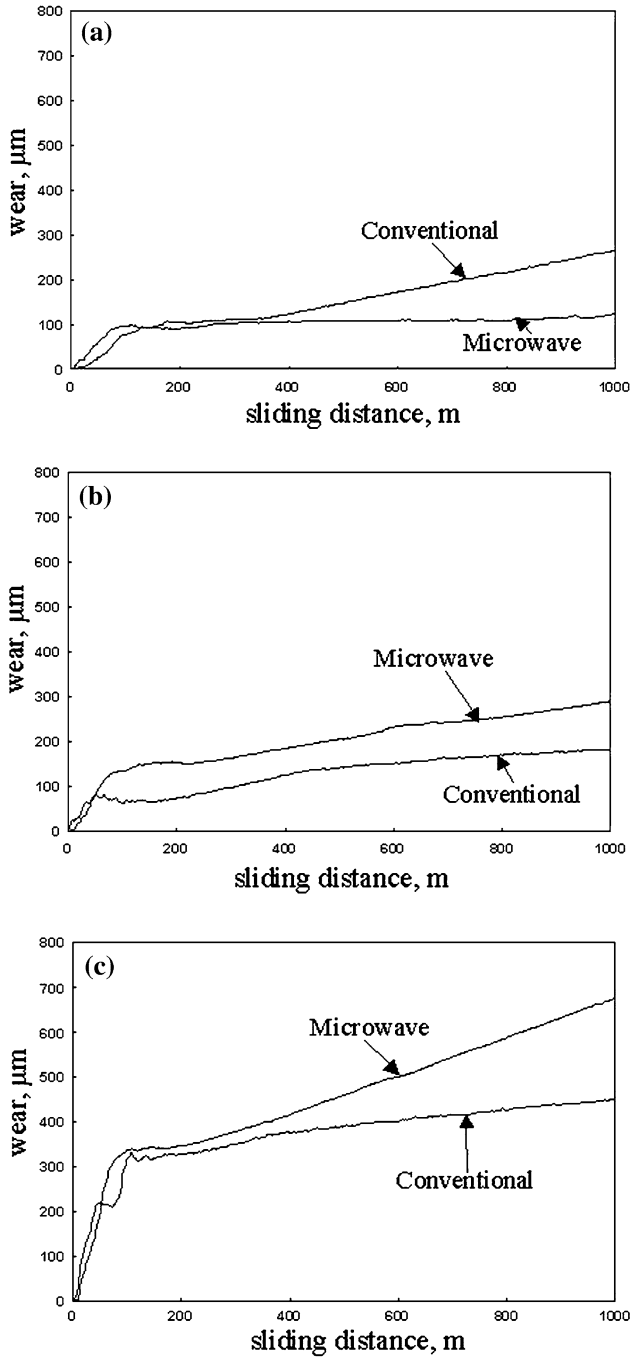

Fig. 10 Effect of heating mode on the sliding wear of (**a**) 434L, (**b**) 434L + 5YAG, and (**c**) 434L + 10YAG compacts sintered at 1,400 °C

Sliding wear response

Figure 10a–c compares the sliding wear behavior of 434L, 434L–5YAG and 434L–10YAG compacts, respectively, sintered at 1,400 °C in conventional and microwave furnace. From the graphs, it is evident that except straight 434L stainless steel, microwave sintering degrades the wear resistance of 434L–YAG compacts. The increase in the wear rate of microwave sintered YAG containing compacts—despite their higher density—can be attributed to poor interfacial bonding between 434L and 434L–YAG particles. Figure 11 compare the wear-tracks of microwave and conventionally sintered 434L and 434L–YAG compacts. Note that YAG addition results in more debris

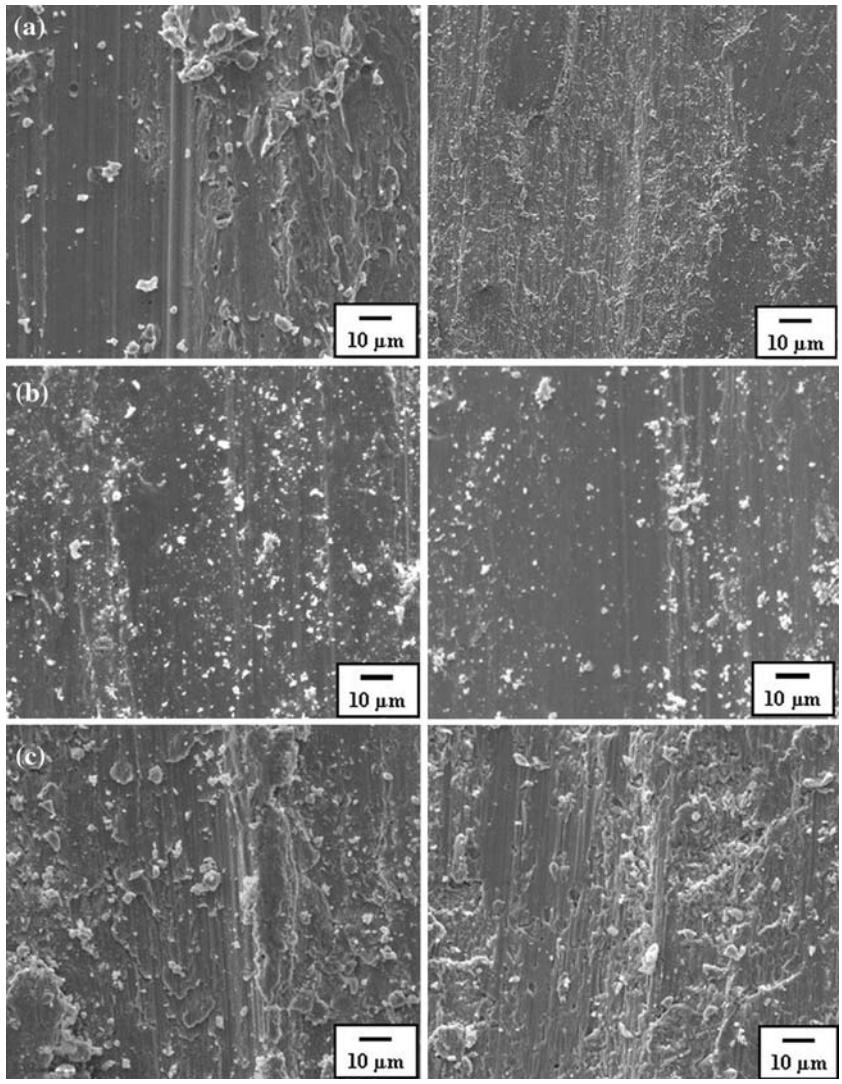

Fig. 11 Wear-tracks of (**a**) 434L, (**b**) 434L + 5YAG, and (**c**) 434L + 10YAG compacts sintered at 1,400 °C in conventional (left) and microwave (right) furnace

in the wear track in microwave sintered compacts. This could be attributed to the presence of elongated, sharp-edged porosity, which act as stress concentration points. Consequently, addition of YAG degrades the wear resistance of microwave sintered 434L compacts. At the same time, straight 434L stainless steel shows better wear resistance than its conventionally sintered counterpart and shows relatively less wear tracks (Fig. 11b). It may be correlated with higher densification of microwave sintered ferritic stainless steel (Fig. 2b) and its refined microstructure (Table 3).

Conclusions

In the present study, the effect of conventional and microwave heating; sintering temperature; and YAG addition on the densification, microstructural, mechanical and tribological properties of 434L ferritic stainless steel is compared. For the first time, it has been shown that both straight 434L as well 434L–YAG composites can be consolidated through solid-state as well as supersolidus sintering using a multimode microwave furnace. About 85% reduction of sintering time is observed in a microwave furnace as compared to conventional furnace heating. Despite their reduced processing time, the microwave sintered compacts in general exhibit higher density and hardness as compared to their conventionally sintered counterparts. This can be attributed to lesser microstructural coarsening during microwave sintering. At supersolidus sintering temperature, YAG addition has almost same effect on densification as that of the straight 434L stainless steel. Pore shape quantification reveals that microwave sintered ferritic stainless steel has more irregular porosity as compared to conventional sintered ones. This results in poor tensile strength, ductility and wears resistance in microwave sintered

compacts. However, straight 434L microwave sintered compact shows better wear resistance than its microwave sintered counterpart which fallow the densification trend. For conventional sintering, up to 5 wt% YAG addition reduces sinterability of 434L compacts and thereby degrades its ductility. In contrast, 434L–10YAG composite exhibit higher densification during microwave sintering, which, in turn, results in higher hardness, ductility, and strength. However, the wear resistance of YAG-added stainless compacts sintered using microwave is relatively lower than their conventionally sintered counterparts.

Acknowledgements The authors gratefully acknowledge the financial support from Department of Science & Technology (DST) and Ministry of Human Resource and Development (MHRD), India. The microwave sintering experiments were conducted at the Microwave Research Center at Penn Sate University through partial financial support from DOE (grant no. DE-FC26-02NT41662). Assistance provided by Vintee Singh in experiments is also gratefully acknowledged.

References

1. Davis JR (1994) In: Stainless steels. ASM International, Materials Park, OH, USA
2. Dyke DL, Ambs HD (1983) In: Klar E (ed) American society for metals, powder metallurgy applications, advantages and limitations. ASM, Materials Park, OH, USA, p 123
3. German RM (ed) (1998) Powder metallurgy of iron and steel. John Wiley, New York, NY, USA
4. German RM (ed) (1996) Sintering theory and practice. John Wiley, New York, NY, USA
5. Madan DS (1991) Int J Powder Metall 27:339
6. Lei G, German RM, Nayar HS (1983) Powder Metall Int 15:70
7. Chatterjee SK, Warwick ME (1985) In: Modern developments in powder metallurgy, vol 16 MPIF, Princeton, NJ, USA, p 277
8. Wang W, Su Y (1986) Powder Metall 29:177
9. Molinari A, Strafelini G, Kazior J, Pieczonka T (1998) Int J Powder Metall 34:21
10. Reinshagen JH, Mason RP (1994) Int J Powder Metall 30:165
11. Cambal L, Lund JA (1972) Int J Powder Metall 8:131
12. German RM (1997) Metall Mater Trans A 28:1553
13. German RM (1997) Int J Powder Metall 33:49
14. Pagounis E, Lindroos VK (1998) Mater Sci Eng A 246:221
15. Velasco F, Anton N, Torralba JM, Ruiz-Prieto JM (1997) Mater Sci Tech 13:847
16. Patankar SN, Tan MJ (2000) Powder Metall 43:350
17. Datta P, Upadhyaya GS (2003) Sci Sintering 32:109
18. Vardavoulias M, Jeandin M, Velasco F, Torralba JM (1996) Tribol Int 29:499
19. Mukherjee SK, Upadhyaya GS (1983) Int J Powder Metall Powder Tech 19:289
20. Shankar J, Upadhyaya A, Balasubramaniam R (2004) Corr Sci 46:487
21. Jain J, Kar AM, Upadhyaya A (2004) Mater Lett 58:2037
22. Rao KJ, Ramesh PD (1995) Bull Mater Sci 18:447
23. Clark DE, Sutton WH (1996) Ann Rev Mater Sci 26:299
24. Pozar DM (ed) (2001) Microwave engineering, 2nd edn. John Wiley, Toronto, Canada
25. Gerdes T, Willert-Porada M, Rödiger K, Dreyer K (1996) Mater Res Soc Symp Proc 430:175
26. Roy R, Agrawal DK, Cheng JP, Gedevanishvili S (1999) Nature 399:668
27. Willert-Porada M, Park HS (2001) In: Clark DE, Binner JGP, Lewis DA (eds) Microwaves: theory and application in materials processing IV. The American Ceramic Society, Westerville, OH, USA, p 459
28. Anklekar RM, Agrawal DK, Roy R (2001) Powder Metall 44:355
29. Sethi G, Upadhyaya A, Agrawal D (2003) Sci Sintering 35:49
30. Willert-Porada M (1997) In: Clark DE, Sutton WH, Lewis DA (eds) Microwaves: theory and application in materials processing IV. The American Ceramic Society, Westerville, OH, USA, p 153
31. Standard Test Methods For Metal Powders and Powder Metallurgy Products (1991) Metal Powder Industries Federation, Princeton, NJ, USA
32. Pert E, Carmel Y, Birnboim A, Olorunyolemi T, Gershon D, Calame J, Lloyd IK, Wilson Jr OC (2001) J Am Ceram Soc 84:1981
33. Lide DR (ed) (1998) CRC handbook of chemistry and physics, 79th edn. CRC Press, Boca Raton, FL, USA
34. Nayer A (ed) (1997) The metals data book. McGraw-Hill, New York, NY, USA
35. Howard RT, Cohen M (1947) Trans AIME 172:413
36. Mishra P, Sethi G, Upadhyaya A (2006) Metall Mater Trans B 37B:839
37. Kang SJL (ed) (2005) Sintering: densification, grain growth & microstructure. Elsevier Butterworth-Heinemann, London, UK
38. Sahay SS, Krishan K (2004) Physica B 348:310
39. Sahay SS, Krishnan K (2005) Thermochim Acta 430:23
40. Peelamedu RD, Roy R, Agrawal D (2001) Mater Res Bull 36:2723
41. Anklekar RM, Bauer K, Agrawal DK, Roy R (2005) Powder Metall 48:39
42. Iglesias FAC, Roman JMR, Cambronero LEG, Prieto JMR, Lopez ERM, Lopez FA (1998) In: Proc of PM World Congress: high alloy steel, vol. 3. EPMA, Shrewsbury, UK, p 471